

Studies of the K_{e4} decay at NA48

Michal Zamkovsky^{*†}

Charles University, Prague

E-mail: michal.zamkovsky@cern.ch

The NA48/2 experiment has recently published a detailed study of the K_{e4} decay mode $K \rightarrow \pi^0 \pi^0 e \nu$ based on 65000 candidates with a low 1% background contamination. The achieved experimental precision brings evidence for isospin breaking mass effects and final state $\pi - \pi$ scattering. Theoretical calculations will have to face a new precision challenge when using such improved inputs to extract for example low energy constants of Chiral Perturbation Theory.

The 8th International Workshop on Chiral Dynamics

29 June 2015 - 03 July 2015

Pisa, Italy

^{*}Speaker.

[†]for the NA48/2 Collaboration: Cambridge, CERN, Dubna, Chicago, Edinburgh, Ferrara, Firenze, Mainz, North-western, Perugia, Pisa, Saclay, Siegen, Torino, Wien

1. Introduction

K_{e4} decays provide a perfect tool for studying low energy QCD and short-range pion interactions. There is K_{e4}^{+-} mode with charged pions in the final state and neutral K_{e4}^{00} with two π^0 s. As the first mode is already discussed in [1], this report will focus on the neutral mode. Very limited information is available from studies of a total of 37 observed K_{e4}^{00} events in three different experiments [3],[4],[5] combined in a branching ratio value of $(2.2 \pm 0.4) \times 10^{-5}$ [6]. No form factor determination has been done so far, only a relation between partial rate and a constant form factor value $\Gamma = (0.75 \pm 0.05)|V_{us} \cdot F|^2 \cdot 10^3 \text{s}^{-1}$, with $|V_{us} \cdot F| = 1.54 \pm 0.15$ has been evaluated. The more recent experiment E470 at KEK [7] observed 214 such decays from stopped kaons in an active target but this result had an error dominated by systematics which hindered its gain in statistical precision.

The theoretical predictions based on isospin symmetry relate more precisely measured modes and predict: $\Gamma(K_{l4}^{+-}) = 1/2\Gamma(K_{l4}^{0\pm}) + 2\Gamma(K_{l4}^{00})$, where $l = e, \mu$ and $K_{l4}^{0\pm}$ denotes the $K \rightarrow \pi^0 \pi^{\pm} l^{\pm} \nu$ decay mode. Considering the different lifetimes τ_{K^+} , τ_{K^0} , this results in:

$$\text{BR}(K_{e4}^{+-}) - 2\text{BR}(K_{e4}^{00}) - \frac{1}{2}\text{BR}(K_{e4}^{0\pm}) \frac{\tau_{K^{\pm}}}{\tau_{K^0}} = (-0.772 \pm 0.801) \cdot 10^{-2}$$
, where the error is dominated by K_{e4}^{00} (1–2)% relative precision for K_{l4}^{+-} and $K_{l4}^{0\pm}$ while K_{e4}^{00} is known to 18% only. Chiral Perturbation Theory (χ PT) calculations $O(p^2, p^4, p^6)$ from Bijens, Colangelo and Gasser from 1994 [8] using the leading partial wave contribution to the decay amplitude from K_{e4}^{+-} form factors from 1977 predicts: $\text{BR}(K_{e4}^{00}) = (2.01 \pm 0.11) \cdot 10^{-5}$, where the 5% relative error comes from the form factors experimental precision in [9].

A large sample of 65000 K_{e4}^{00} decays has been collected by the NA48/2 experiment at CERN. Based on this sample, both branching ratio and form factor measurements were obtained with improved precision [2].

2. Physical motivation

The most general K_{l4} decay is fully described by five kinematical variables. It is convenient to consider the kaon rest frame, the dipion rest frame and the dilepton rest frame and then use the Cabibbo-Maksymowicz variables [11]:

- $S_{\pi} = M_{\pi\pi}^2$, the square of the dipion invariant mass,
- $S_e = M_{e\nu}^2$, the square of the dilepton invariant mass,
- θ_{π} , the angle of one π^0 in the dipion rest frame with respect to the flight direction of the dipion in the K^{\pm} rest frame,
- θ_e , the angle of the e^{\pm} in the dilepton rest frame with respect to the flight direction of the dilepton in the K^{\pm} rest frame,
- ϕ , the angle between the dipion and dilepton rest frames.

The definition of angles is shown in figure 1.

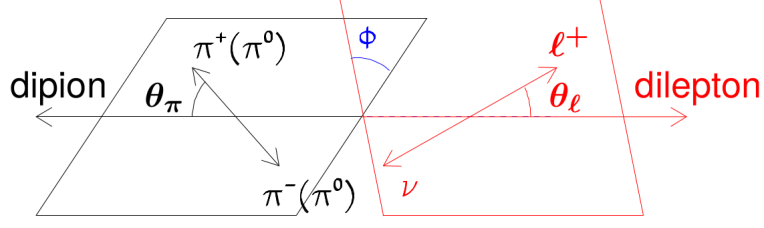


Figure 1: Topology of the charged K^+ decay showing the angle definitions.

The decay probability summed over lepton spins in Cabibbo-Maksymowicz variables can be written as [8]:

$$d^5\Gamma = \frac{G_F^2 |V_{us}|^2}{2(4\pi)^6 m_K^5} \rho(S_\pi, S_e) J_5(S_\pi, S_e, \cos \theta_\pi, \cos \theta_e, \phi) \times dS_\pi dS_e d\cos \theta_\pi d\cos \theta_e d\phi, \quad (2.1)$$

where $\rho(S_\pi, S_e)$ is the phase space factor $\frac{1}{2} \lambda^{1/2}(m_K^2, S_\pi, S_e) \sigma(S_\pi)(1 - z_e)$, with $z_e = m_e^2/S_e$,

$\lambda(a, b, c) = a^2 + b^2 + c^2 - 2ab - 2ac - 2bc$ and $\sigma(s) = \sqrt{1 - \frac{4m_\pi^2}{s}}$.

The function J_5 is defined as [12]:

$$J_5 = 2(1 - z_e) (I_1 + I_2 \cos 2\theta_e + I_3 \sin^2 \theta_e \cdot \cos 2\phi + I_4 \sin 2\theta_e \cdot \cos \phi + I_5 \sin \theta_e \cdot \cos \phi + I_6 \cos \theta_e + I_7 \sin \theta_e \cdot \sin \phi + I_8 \sin 2\theta_e \cdot \sin \phi + I_9 \sin^2 \theta_e \cdot \sin 2\phi), \quad (2.2)$$

where

$$\begin{aligned} I_1 &= \frac{1}{4} \left[(1 + z_e) |F_1|^2 + \frac{1}{2} (3 + z_e) (|F_2|^2 + |F_3|^2) \sin^2 \theta_\pi + 2z_e |F_4|^2 \right], \\ I_2 &= -\frac{1}{4} (1 - z_e) \left[|F_1|^2 - \frac{1}{2} (|F_2|^2 + |F_3|^2) \sin^2 \theta_\pi \right], \\ I_3 &= -\frac{1}{4} (1 - z_e) (|F_2|^2 + |F_3|^2) \sin^2 \theta_\pi, \\ I_4 &= \frac{1}{2} (1 - z_e) \text{Re}(F_1^* F_2) \sin \theta_\pi, \\ I_5 &= -[\text{Re}(F_1^* F_3) + z_e \text{Re}(F_4^* F_2)], \\ I_6 &= -[\text{Re}(F_2^* F_3) \sin^2 \theta_\pi - z_e \text{Re}(F_1^* F_4)], \\ I_7 &= -[\text{Im}(F_1^* F_2) + z_e \text{Im}(F_4^* F_3)], \\ I_8 &= \frac{1}{2} (1 - z_e) \text{Im}(F_1^* F_3) \sin \theta_\pi, \\ I_9 &= -\frac{1}{2} (1 - z_e) \text{Im}(F_2^* F_3) \sin^2 \theta_\pi, \end{aligned} \quad (2.3)$$

where $F_i, i = 1 \dots 4$ are combinations of hadronic form factors F, G, H, R :

$$\begin{aligned} F_1 &= X \cdot F + \sigma(S_\pi)(PL) \cos \theta_\pi \cdot G, \\ F_2 &= \sigma(S_\pi) (S_\pi S_l)^{1/2} G, \\ F_3 &= \sigma(S_\pi) (S_\pi S_l)^{1/2} \frac{H}{m_K^2}, \\ F_4 &= -(PL)F - S_l R - \sigma(S_\pi)X \cos \theta_\pi \cdot G, \end{aligned} \quad (2.4)$$

where $X = \frac{1}{2} \lambda^{1/2}(m_K^2, S_\pi, S_e)$ and PL is a dot product of four momentum sums of two pions (P) and two leptons (L). In K_{e4} decays, the electron mass can be neglected ($z_e = 0$) and the terms $(1 \pm z_e)$ become unity. Notice that the form factor F_4 is always multiplied by z_e and thus does not contribute to the full expression, neither does R . These terms will contribute significantly only to $K_{\mu 4}$ decays.

If T-invariance holds, the Watson theorem [13] tells us that the partial-wave amplitude of definite angular momentum l and isospin I must have the phase of the corresponding $\pi\pi$ amplitude δ_l^I .

Developing further F_1, F_2, F_3 in a partial wave expansion with respect to the variable $\cos \theta_\pi$ using Legendre functions $P_l(\cos \theta_\pi)$ and their derivative $P_l'(\cos \theta_\pi)$,

$$\begin{aligned} \frac{F_1}{m_K^2} &= \sum_{l=0}^{\infty} P_l(\cos \theta_\pi) F_{1,l} e^{i\delta_l}, \\ \frac{F_{2(3)}}{m_K^2} &= \sum_{l=0}^{\infty} P_l'(\cos \theta_\pi) F_{2(3),l} e^{i\delta_l}, \end{aligned} \quad (2.5)$$

one can now express the form factors F, G, H using explicitly the modulus and phase of each complex contribution. A D-wave contribution would appear as a $\cos^2 \theta_\pi$ term for F and $\cos \theta_\pi$ terms for G, H with its own phase:

$$\begin{aligned} F &= F_s e^{i\delta_{fs}} + F_p e^{i\delta_{fp}} \cos \theta_\pi + F_d e^{i\delta_{fd}} \cos^2 \theta_\pi, \\ G &= G_p e^{i\delta_{gp}} + G_d e^{i\delta_{gd}} \cos \theta_\pi, \\ H &= H_p e^{i\delta_{hp}} + H_d e^{i\delta_{hd}} \cos \theta_\pi. \end{aligned} \quad (2.6)$$

For K_{e4}^{00} decays, due to the presence of two identical particles, the π^0 system cannot be in a $l = 1$ state and the expansion includes only S- and D-wave terms. In the first approximation, only the S-wave term contributes and the form factor F_s can be parametrized as [14]:

$$F_s = \left(f_s + f_s' q_0^2 + f_s'' q_0^4 + f_e \left(\frac{S_e}{4m_{\pi^0}^2} \right) \right) e^{i\delta_0^0}, \quad (2.7)$$

where $q_0 = \sqrt{\frac{S_\pi - 4m_{\pi^0}^2}{4m_{\pi^0}^2}}$. This parametrization leads to four dimensionless parameters (f_s, f_s', f_s'', f_e) , which unlike the form factor do not depend on kinematical variables. After integrating the expression of J_5 (2.2) over $\cos \theta_\pi$ and ϕ one obtains:

$$J_3 = |XF_s|^2 (1 - \cos 2\theta_e) = 2|XF_s|^2 \sin^2 \theta_e, \quad (2.8)$$

and the differential rate:

$$d^3\Gamma = \frac{G_F^2 |V_{us}|^2}{2(4\pi)^6 m_K^5} \rho(S_\pi, S_e) J_3(S_\pi, S_e, \cos \theta_e) \times dS_\pi dS_e d\cos \theta_e. \quad (2.9)$$

After performing integration over θ_e the connection between remaining variables S_π, S_e and measured parameters (f_s, f'_s, f''_s, f_e) can be seen.

3. Experimental setup

The primary 400 GeV/c SPS proton beam impinging on a beryllium target produces two simultaneous K^\pm beams with a central momentum of (60 ± 3) GeV/c. The secondary beams are focused ~ 200 m downstream at the first spectrometer chamber with transverse size ~ 10 mm. The decay volume housed in a 114 m long evacuated vacuum tank is followed by a magnetic spectrometer (a dipole magnet surrounded by two sets of drift chambers) located in a tank filled with helium at nearly atmospheric pressure. The momentum resolution achieved in the spectrometer is $\sigma_p/p = (1.02 \oplus 0.044 \cdot p)\%$ (p in GeV/c) and spatial resolution is $\sigma_x = \sigma_y = 90\mu\text{m}$. The spectrometer is followed by a scintillator hodoscope consisting of two planes segmented into horizontal and vertical strips achieving a very good ~ 150 ps time resolution. A liquid krypton calorimeter (LKr) measures the energy of electrons and photons. The transverse segmentation into 13248 $2\text{ cm} \times 2\text{ cm}$ projective cells and the 27 radiation length thickness result in an energy resolution $\sigma(E)/E = (3.2/\sqrt{E} \oplus 9.0/E \oplus 0.42)\%$ (E in GeV/c) and a transverse position resolution 1.5 mm for 10 GeV showers. This allows to separate electrons ($E/p \sim 1$) from pions ($E/p < 1$). A two-level trigger logic selected and flagged events with a high efficiency for both K_{e4} decay modes. A detailed description is available in [10].

4. Event selection

The K_{e4}^{00} candidates are reconstructed from one charged track and four photons from π^0 's pointing to the same vertex. The events for signal K_{e4}^{00} and normalization $K_{3\pi}^{00}$ ($K \rightarrow \pi^\pm \pi^0 \pi^0$) modes are selected concurrently as far as possible to reduce systematic effects coming from beam modeling imperfections. Then the separation between signal and normalization candidates is based on the missing transverse momentum (p_t), as $K_{3\pi}^{00}$ is fully reconstructed and K_{e4}^{00} has some missing p_t due to the undetected neutrino, and the invariant mass with charged pion assumption. The reconstructed $M_{3\pi}^{00}$ mass should be consistent with the kaon mass for fully reconstructed $K_{3\pi}^{00}$ events and mostly inconsistent for K_{e4}^{00} events. Using both variables, elliptic cuts in the plane $(M_{3\pi} - M_K, p_t)$ have been introduced for a better separation as illustrated in figure 2.

Extra requirements of electron identification are then applied:

- charged track momentum larger than 5 GeV/c;
- E/p ratio of associated energy cluster E in LKr calorimeter and momentum p measured in the spectrometer is within $(0.9, 1.1)$;
- further suppression of pions mis-identified as electrons is obtained by using a discriminant variable related to shower properties.

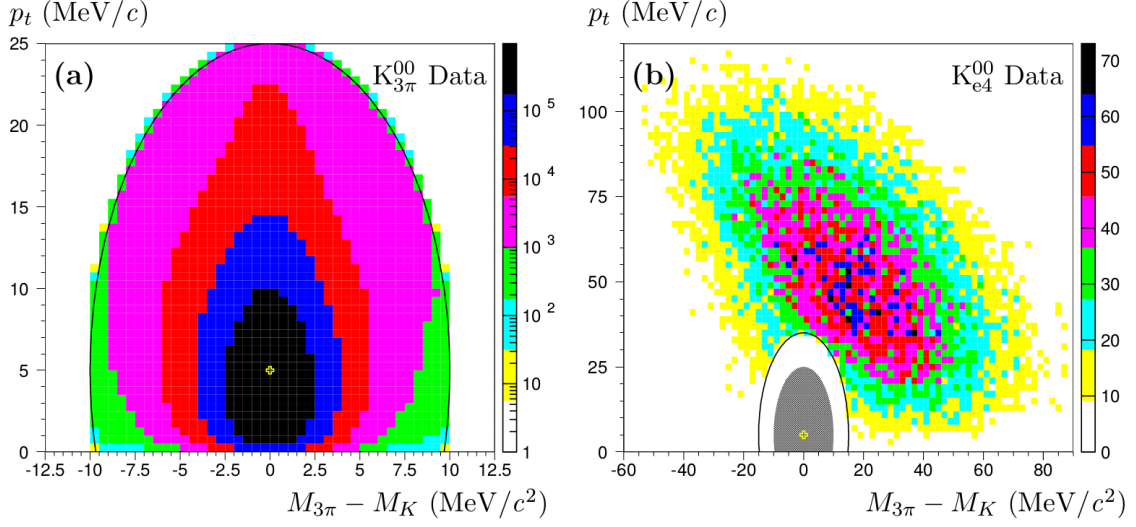


Figure 2: Distribution of events in the plane $(M_{3\pi} - M_K, p_t)$ for $K_{3\pi}^{00}$ (left) and K_{e4}^{00} (right).

The main sources of background to the K_{e4}^{00} decay are:

- fake-electrons from pions in $K_{3\pi}^{00}$ decays;
- genuine electrons/positrons from $K_{3\pi}^{00}$ followed by $\pi \rightarrow e\nu$ decay ($\sim 8\%$ of these π^\pm do decay, mostly to $\mu^\pm\nu$ while $\text{BR}(\pi e\nu) = 1.23 \times 10^{-4}$);
- accidental coincidence of another kaon decay with an additional track or photon resulting in the same final state topology as the signal.

The first and the third contributions are measured on data samples, while for the second dedicated simulation has been produced to achieve better statistics. The relative contributions from these background sources are 0.65% for the first source, 0.12% from the second source and 0.22% for the accidentals. It results into the background (B) to signal (S) ratio: $B/(S+B) = 1.00\%$.

5. Form factor measurement

The event density in the Dalitz plot (the plane (S_π, S_e)) is proportional to the S-wave axial vector form factor F_s^2 and its variation is used to determine the form factor coefficients f_s', f_s'' and f_e . These values are given relative to a common value f_s , which can be obtained using the branching ratio measurement. After background subtraction, the Dalitz plot is compared to the simulated events generated with a flat form factor taking into account acceptance, resolution, trigger efficiency and radiative effects using PHOTOS [15]. Figure 3 displays the (S_π, S_e) plane and the projected distributions after background subtraction for data.

The ratio of the populations Data/MC is fitted in the plane $(q^2, \frac{S_e}{4m_{\pi^+}^2})$, using the charged pion mass instead of the neutral one to define dimensionless variables same as in the K_{e4}^{00} mode, enabling

the direct comparison of the form factor. The fitting function is a series expansion above $q^2 = 0$ and an empirical function below:

$$F_s = \left(1 + aq^2 + bq^4 + c \left(\frac{S_e}{4m_{\pi^+}^2} \right) \right) \quad q^2 \geq 0, \quad (5.1)$$

$$F_s = \left(1 + d\sqrt{|q^2/(1+q^2)|} + c \left(\frac{S_e}{4m_{\pi^+}^2} \right) \right) \quad q^2 < 0, \quad (5.2)$$

where the parameter c is same for both functions as the variation of q^2 is affecting only S_π axis of Dalitz plot, not S_e . The fit result projected on the q^2 axis is illustrated in figure 4. A cusp-like singularity is observed at $q^2 = (S_\pi/4m_{\pi^+}^2 - 1) = 0$.

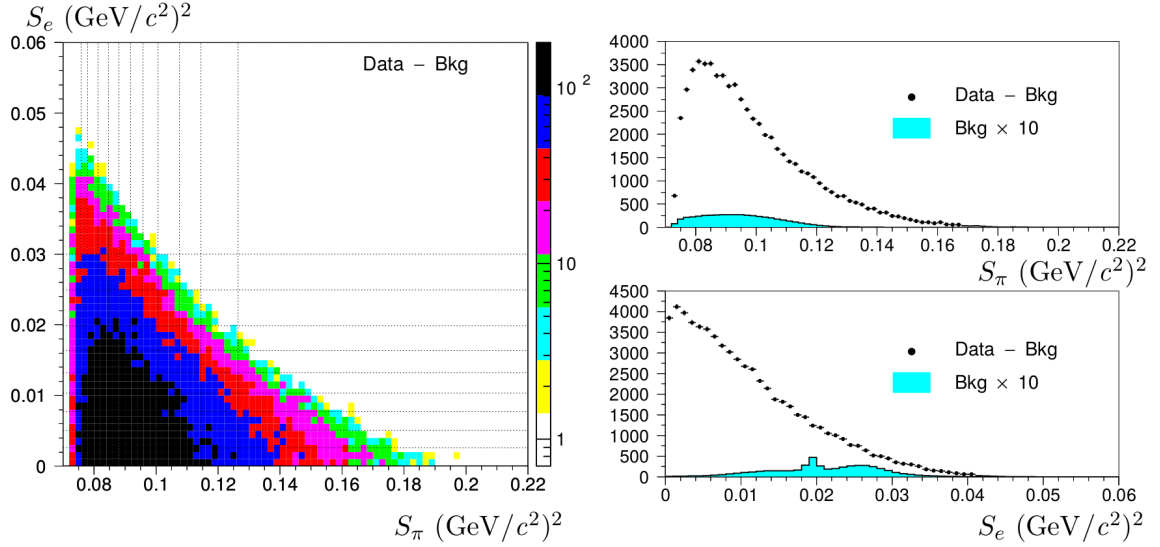


Figure 3: Event density in the Dalitz plot and corresponding projections with displayed background occupancies.

The fit results are obtained as:

$$\begin{aligned} a &= 0.149 \pm 0.033 & b &= -0.070 \pm 0.039 \\ c &= 0.113 \pm 0.022 & d &= -0.256 \pm 0.049 \end{aligned} \quad (5.3)$$

The results in the $(q^2, S_e/4m_{\pi^+}^2)$ formulation can be directly compared to those obtained in the K_{e4}^{+-} analysis [1] where the corresponding form factor is described as $F_s = f_s(1 + f'_s/f_s q^2 + f''_s/f_s q^4 + f'_e/f_s \frac{S_e}{4m_{\pi^+}^2})$ and are shown in figure 5.

The observed cusp singularity can be identified with the charge exchange reaction $\pi^+\pi^- \rightarrow \pi^0\pi^0$, which is directly proportional to the $a_0 - a_2$ combination of the $\pi - \pi$ S-wave scattering lengths [16]. In case of conserved isospin symmetry ($m_{\pi^+} = m_{\pi^0}$), we have following description:

$$\mathcal{M}_1 = -2 \frac{a_0^0 - a_2^0}{3} f_s \sqrt{\left| \frac{q^2}{1+q^2} \right|}, \quad q^2 = \frac{S_\pi - 4m_{\pi^+}^2}{4m_{\pi^+}^2}, \quad (5.4)$$

but in case of broken isospin symmetry ($m_{\pi^+} \neq m_{\pi^0}$) we need a more elaborate calculation as developed for example in [17].

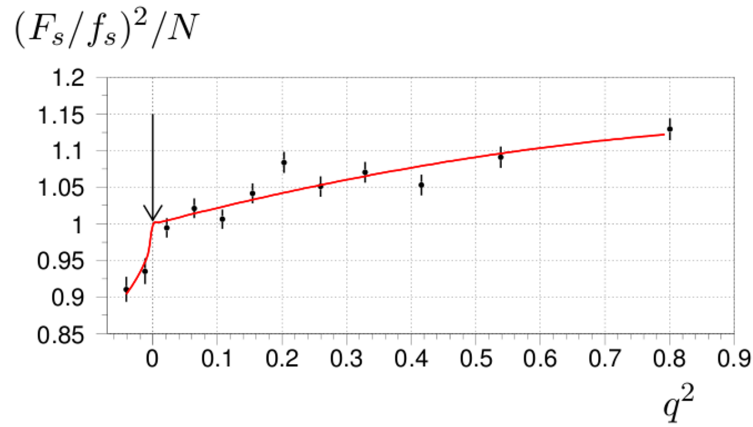


Figure 4: Ratio of the two q^2 distributions (data over MC with flat form factor) in equal population bins. Each symbol is plotted at the barycenter position of the data events in the bin to account correctly for the variable size binning. The line corresponds to the empirical description using the best fit-parameter values: a degree-2 polynomial above $q^2 = 0$ and a cusp-like function below.

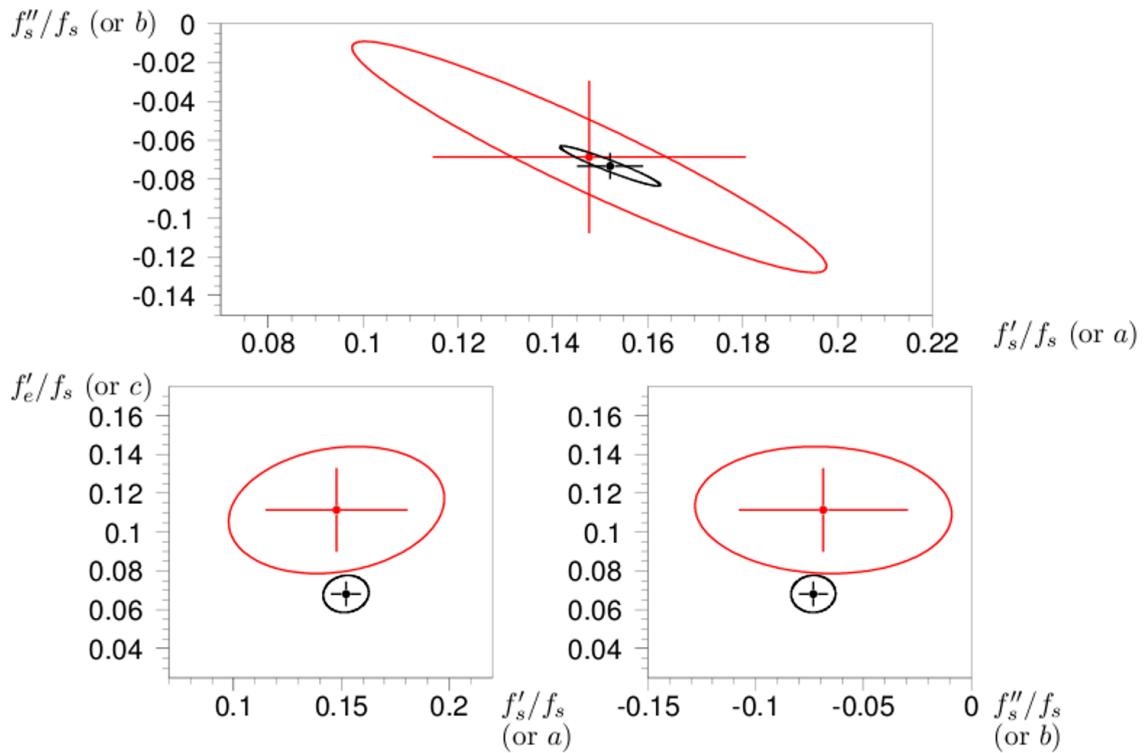


Figure 5: Form factor comparison of K_{e4}^{+-} and K_{e4}^{00} modes. Errors plotted are statistical only and all contours are 68% CL. The smaller area (black ellipses) corresponds to the K_{e4}^{+-} result obtained from a large statistical sample [1]. The correlations between fitted parameter errors are very similar and results are consistent within statistical errors.

6. Branching ratio measurement

The branching ratio is measured relatively to the abundant $K_{3\pi}^{00}$ mode, which is collected concurrently with the same trigger logic. This approach is minimizing systematic effects which partially cancel between signal and normalization:

$$\text{BR}(K_{e4}^{00}) = \frac{N(K_{e4}^{00}) - N_{Bkg}(K_{e4}^{00})}{N(K_{3\pi}^{00}) - N_{Bkg}(K_{3\pi}^{00})} \cdot \frac{A(K_{3\pi}^{00})}{A(K_{e4}^{00})} \cdot \frac{\varepsilon(K_{3\pi}^{00})}{\varepsilon(K_{e4}^{00})} \cdot \text{BR}(K_{3\pi}^{00}), \quad (6.1)$$

where $N(K_{e4}^{00})$ and $N_{Bkg}(K_{e4}^{00})$ ($N(K_{3\pi}^{00})$ and $N_{Bkg}(K_{3\pi}^{00})$) are the numbers of candidates for signal and background (normalization), $A(K_{e4}^{00})$ ($A(K_{3\pi}^{00})$) and $\varepsilon(K_{e4}^{00})$ ($\varepsilon(K_{3\pi}^{00})$) geometrical acceptance and trigger efficiency for signal (normalization).

The BR of the normalization mode $\text{BR}(K_{3\pi}^{00}) = (1.761 \pm 0.022) \times 10^{-2}$ is taken from PDG tables [6].

In total 65210 K_{e4}^{00} signal and almost hundred million normalization events were reconstructed in ten statistically independent samples (data taking periods) and the combined branching ratio is:

$$\text{BR}(K_{e4}^{00}) = (2.552 \pm 0.010_{stat} \pm 0.010_{syst} \pm 0.032_{ext}) \times 10^{-5}.$$

7. Conclusion

From a sample of $\sim 65000 K_{e4}^{00}$ reconstructed events, the branching ratio has been measured to be:

$$\text{BR}(K_{e4}^{00}) = (2.552 \pm 0.010_{stat} \pm 0.010_{syst} \pm 0.032_{ext}) \times 10^{-5}$$

using $K_{3\pi}^{00}$ decay as a normalization mode.

This measurement improves over the previous K_{e4}^{00} branching ratio measurements by one order of magnitude while the error is now dominated by the external uncertainty from the normalization mode.

The first measurement of the form factor F_s parametrized by described a, b, c, d constants is obtained from the fit in the (S_π, S_e) plane. The results are:

$$\begin{aligned} a &= 0.149 \pm 0.033 & b &= -0.070 \pm 0.039 \\ c &= 0.113 \pm 0.022 & d &= -0.256 \pm 0.049. \end{aligned}$$

The observed cusp-like singularity which can be related to $\pi - \pi$ scattering is consistent with a_0^0, a_2^0 values measured in K_{e4}^{+-} mode.

References

- [1] J. Batley *et al.*, Eur. Phys. J. **C70** (2010) 635.
- [2] J. Batley *et al.*, JHEP **08** (2014) 159.
- [3] D. Cline and Q. Ljung, Phys. Lett. **28** (1972) 1287.
- [4] V. Bolotov *et al.*, Sov. J. Nucl. Phys. **44** (1986) 68.

- [5] V. Barmin et al., Sov. J. Nucl. Phys. **48** (1988) 1032.
- [6] K.A. Olive *et al.* (Particle Data Group), Chin. Phys. C, **38**, 090001 (2014).
- [7] S. Shimizu *et al.*, Phys. Rev. **D70** (2004) 037101.
- [8] J. Bijnens, G. Colangelo and J. Gasser, Nucl. Phys. B **427** (1994) 427 [hep-ph/9403390].
- [9] S118: L. Rosselet et al., Phys. Rev. **D15** (1977) 574.
- [10] V. Fanti *et al.*: Nucl. Instrum. Methods A **574**, (2007) 433.
- [11] N. Cabibbo and A. Maksymowicz, Phys. Rev. **137**(1965) B438 [Erratum-ibid. **168** (1968) 1926].
- [12] A. Pais and S. B. Treiman, Phys. Rev. **168** (1968) 1858.
- [13] K. M. Watson, Phys. Rev. **88** (1952) 1163.
- [14] G. Amoros and J. Bijnens, J. Phys. G **25** (1999) 1607 [hep-ph/9902463].
- [15] E. Barbiero and Z. Was, PHOTOS, Comp. Phys. Comm. **79** (1994) 291.
- [16] N. Cabibbo and G. Isidori, JHEP **0503** (2005) 021 [hep-ph/0502130].
- [17] M. Knecht, Isospin breaking effects in the K_{e4} decays, this conference.